

NOAA Technical Memorandum ERL PMEL-28

CIRCULATION IN THE LOWER COOK INLET, ALASKA

R. D. Muench  
J. D. Schumacher  
C. A. Pearson

Pacific Marine Environmental Laboratory  
Seattle, Washington  
July 1981



**UNITED STATES  
DEPARTMENT OF COMMERCE**

**Malcolm Baldrige,  
Secretary**

**NATIONAL OCEANIC AND  
ATMOSPHERIC ADMINISTRATION**

John V. Byrne,  
Administrator

Environmental Research  
Laboratories

Joseph O. Fletcher,  
Acting Director

## NOTICE

The Environmental Research Laboratories do not approve, recommend, nor endorse any proprietary product or proprietary material mentioned in this publication. No reference shall be made to the Environmental Research Laboratories or to this publication furnished by the Environmental Research Laboratories in any advertising or sales promotion which would indicate or imply that the Environmental Research Laboratories approve, recommend, or endorse any proprietary product or proprietary material mentioned herein, or which has as its purpose an intent to cause directly or indirectly the advertised product to be used or purchased because of this Environmental Research Laboratories publication.

## CONTENTS

	Page
Abstract	1
1. Introduction	1
1.1 Geographical Setting	1
1.2 Oceanographic and Meteorological Setting	2
2. Past Research	5
3. Observation Program	6
3.1 Current Meter Moorings	6
3.2 Satellite-Tracked Drifters	6
3.3 Wave Radar (CODAR) Observations	8
3.4 Temperature and Salinity Observations	8
4. Discussion	8
4.1 Mean Circulation and Annual Seasonal Variations	8
4.2 Low-Frequency Current Fluctuations	15
4.3 Tidal Currents	18
5. Summary	18
6. Acknowledgements	23
7. References	24

## FIGURES

- Figure 1. Geographical locations and bathymetry of the lower Cook Inlet region (depths in m). 3
- Figure 2. Schematic of near-surface currents in the northwest Gulf of Alaska region (from Muench and Schumacher, 1980), with currents in the lower Cook Inlet region derived from Muench, Mofjeld, and Charnell (1978). Numbers in parentheses give approximate range of current speeds at that location in cm/s; see text for relation between maximum/minimum values and season. 4
- Figure 3. Locations of taut-wire current moorings deployed in the lower Cook Inlet region during 1977-1978. 7
- Figure 4. Mean current vectors for October 1977 through March 1978. Lengths of arrows indicate current speeds, orientation indicates direction, and numbers near arrowheads indicate observation depths in m. 9
- Figure 5. Mean current vectors for June through October 1978. Lengths of arrows indicate current speeds, orientation indicates direction, and numbers near arrowheads indicate observation depths in m. 12
- Figure 6. Seven-day mean current speeds at middepths (65-70 m) and near-surface (20-25 m) in northern Shelikof Strait at mooring C10 (after Schumacher and Reed, 1980). Mooring location is indicated on figure 3. 14
- Figure 7. Representative segments of low-pass (35-hr) filtered currents from six locations at 20-m depth. Mooring locations are indicated on figure 3. 16
- Figure 8. Mean distribution of horizontal kinetic energy ( $\text{cm}^2/\text{s}^2$ ) at 20- to 25-m depths in two frequency bands; A) 0.03-0.35 cph, which includes semidiurnal and diurnal tidal and inertial energy, and B) 0.001-0.03 cph, which includes prominent low-frequency fluctuations. Parenthesized values were obtained from 63- to 66-m deep observations rather than from 20-25 m. 17
- Figure 9. Trajectories of drogued, satellite-tracked buoys deployed in 1978. Locations are plotted at 1-day intervals. 19
- Figure 10. Example of 24-hr mean surface currents observed in July 1978 using the doppler-shift radar unit discussed by Barrick, Evans, and Weber (1977). Data are courtesy of Dr. A.S. Frisch (Wave Propagation Laboratory, NOAA). 20

## TABLES

- Table 1. Data for lower Cook Inlet current moorings. 10
- Table 2. Tidal current components for four major species derived from current data using the Munk-Cartwright response method (Munk and Cartwright, 1966); H is amplitude (cm/s), G is phase relative to Greenwich ( $^{\circ}$ ), D is direction of major axis ( $^{\circ}$ T), and R is sense of rotation (C for clockwise, A for anticlockwise). 22



# CIRCULATION IN THE LOWER COOK INLET, ALASKA<sup>1</sup>

R. D. Muench,<sup>2</sup> J. D. Schumacher, and C. A. Pearson

## Abstract

Circulation in the lower Cook Inlet region has been described and discussed utilizing current observations obtained during October 1977-October 1978. The major circulation feature was a mean westerly flow which entered the region via Kennedy and Stevenson entrances, paralleled the 100-m isobath through the lower Inlet then exited the system via Shelikof Strait. Summer mean current speeds in this flow were 10-15 cm/s; winter speeds were 25-30 cm/s. A secondary circulation feature was present as southward flow which occupied the western portion of the lower Inlet. Summer current speeds here were 15-20 cm/s, while winter speeds were of order 10 cm/s. The westerly flow is driven in summer primarily by a baroclinic field consequent to coastal freshwater input (the Kenai Current), while in winter this flow is driven to a greater extent by wind-driven coastal convergence and possibly by an alongshore pressure gradient set up by the Alaskan Stream. The southward flow, driven by freshwater input into upper Cook Inlet, therefore is larger in summer when this input is greater. Mean flow in the eastern lower Inlet was weak and variable in all seasons.

Low-frequency and tidal flow fluctuations were superposed upon the mean flow and in regions of low mean speeds controlled the instantaneous flow. The low-frequency fluctuations were associated with westerly flow through the system, and probably originated through meteorological disturbances on the continental shelf outside the Inlet. Tidal currents were large (70-100 cm/s) and primarily semidiurnal in the eastern portion of the lower Inlet and in Kennedy and Stevenson entrances. In the western Inlet, tidal currents were only half this magnitude, and in Shelikof Strait they were very small due to presence of an antinode near the mooring in northern Shelikof Strait. Tidal currents were aligned with the local channel bathymetry.

## 1. Introduction

This paper presents and discusses new data which have allowed a better definition of the regional flow field in the lower Cook Inlet region. These data include current observations from taut-wire moorings, drogued surface buoy trajectories, doppler-shift radar surface current observations, and hydrographic measurements, and were obtained during an intensive field program in 1977-78. This field program was conceived primarily to aid in prediction of spilled contaminant fates and trajectories in light of the projected petroleum exploration and development in lower Cook Inlet.

### 1.1. Geographical Setting

Cook Inlet is a broad (70-90 km), shallow (mean depth about 60 m), elongate embayment protruding northeastward from the confluence of

<sup>1</sup>Contribution No. 531 from the NOAA Pacific Marine Environmental Laboratory

<sup>2</sup>Science Applications, Inc., Bellevue, Washington

Shelikof Strait and Kennedy and Stevenson entrances (fig. 1). The portion which we refer to as lower Cook Inlet is bounded on the north by the Forelands and on the south by Kennedy and Stevenson entrances and northern Shelikof Strait. At the northern end of this region, Kalgin Island and its associated shoals inhibit water flow. In the central portion of the lower Inlet, bottom depths are 60-80 m; depths decrease gradually toward the coastline to the east and west. Depth increases to the south in regular fashion except for a prominent ramplike feature which traverses the Inlet from east to west in arcuate fashion approximately along the 100-m isobath. Maximum depths in the lower Inlet occur in a depression just west of Stevenson Entrance.

The coastline surrounding lower Cook Inlet is extremely mountainous and rises abruptly to elevations of 2000-3000 m along the northern shores of Cook Inlet and Shelikof Strait. The coastal mountains are transected by numerous valleys, many of which contain glaciers or snowfields at their heads.

## 1.2 Oceanographic and Meteorological Setting

The major oceanic circulation feature in the northwest Gulf of Alaska is the Alaskan Stream, a southwestward-flowing current which lies along the shelf break southeast of Kodiak Island (fig. 2). This flow has been characterized by Favorite (1967) on the basis of temperature and salinity data as a western boundary current, which acts as the return flow for the Gulf of Alaska subarctic gyre, and by Thomson (1972) based upon theoretical considerations. Reed (1980) has verified the closed circulation in the Gulf of Alaska gyre using tracks from satellite-tracked, drogued buoys. Peak surface speeds in the Alaskan Stream are of order 100 cm/s, and Reed and Taylor (1965) have presented some evidence that the flow is in geostrophic equilibrium. Ohtani (1970) and Favorite (1974) concluded that there was little seasonal variation in baroclinic transport in the Stream, while Reed, Muench, and Schumacher (1980) came to a similar conclusion and derived a mean annual baroclinic volume transport of  $12 \times 10^6 \text{ m}^3/\text{s}$ .

The prominent shelf circulation feature is the Kenai Current, a 20- to 30-km wide westerly baroclinic coastal flow which is driven by freshwater input from continental drainage (Schumacher and Reed, 1980). This flow originates in the vicinity of the Copper River, east of the lower Cook Inlet region, enters primarily via Kennedy Entrance, and exits to the southwest via Shelikof Strait. It has a large seasonal signal, unlike the Alaskan Stream, varying from a winter low baroclinic volume transport of about  $0.3 \times 10^6 \text{ m}^3/\text{s}$  to an autumn high of about  $1.0 \times 10^6 \text{ m}^3/\text{s}$  with corresponding surface speeds of 15-30 cm/s to more than 100 cm/s.

The shelf region between the Alaskan Stream and the Kenai Current is occupied by Kodiak Island and adjacent banks and is characterized by weak and variable circulation. Despite the intervention of this band of sluggish circulation, Muench, Mofjeld, and Charnell (1978) have speculated that the alongshore pressure gradient associated with the Alaskan Stream drives a significant barotropic volume transport through the lower Cook Inlet system. It now appears, in addition, that at certain



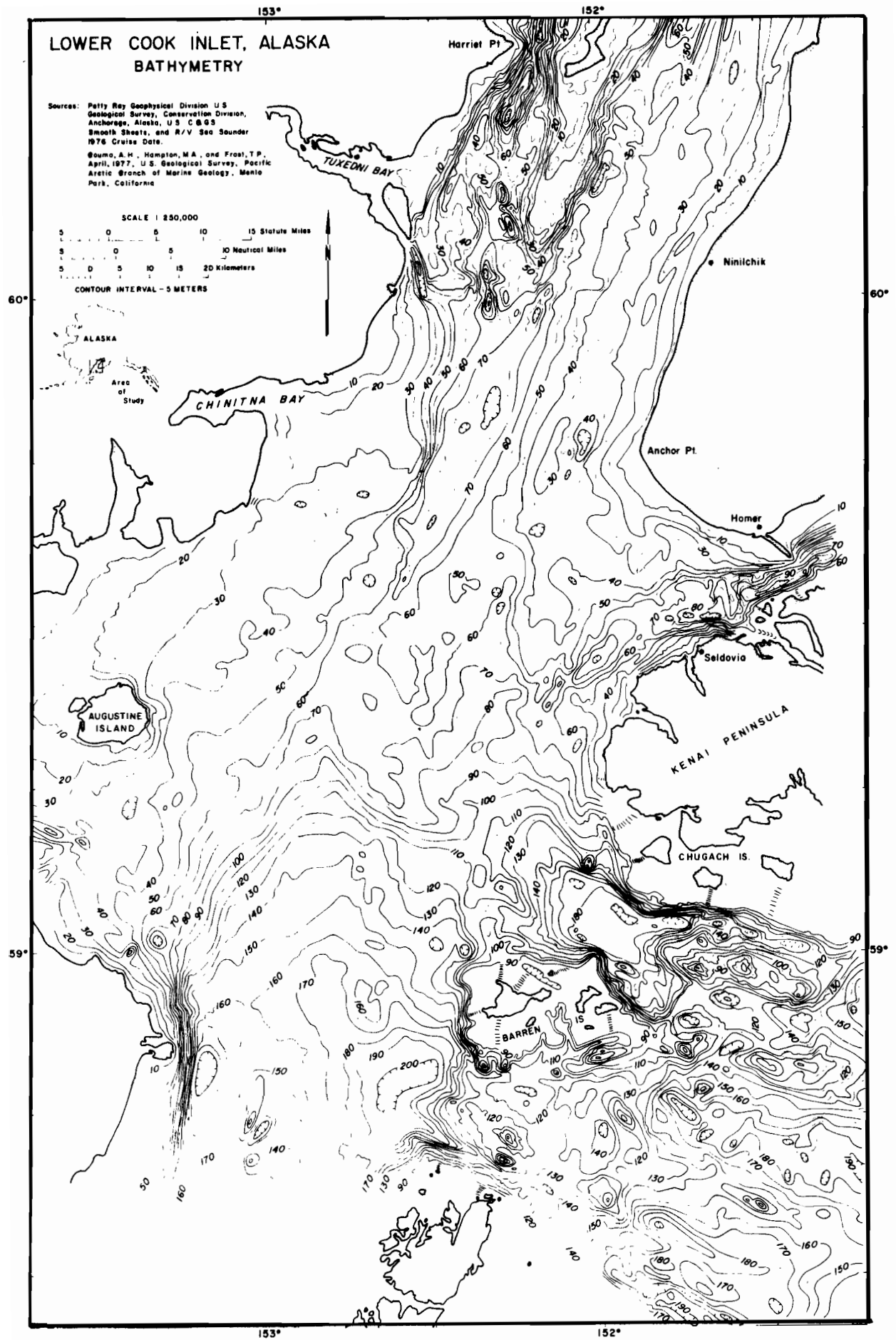


Figure 1. Geographical locations and bathymetry of the lower Cook Inlet region (depths in m).

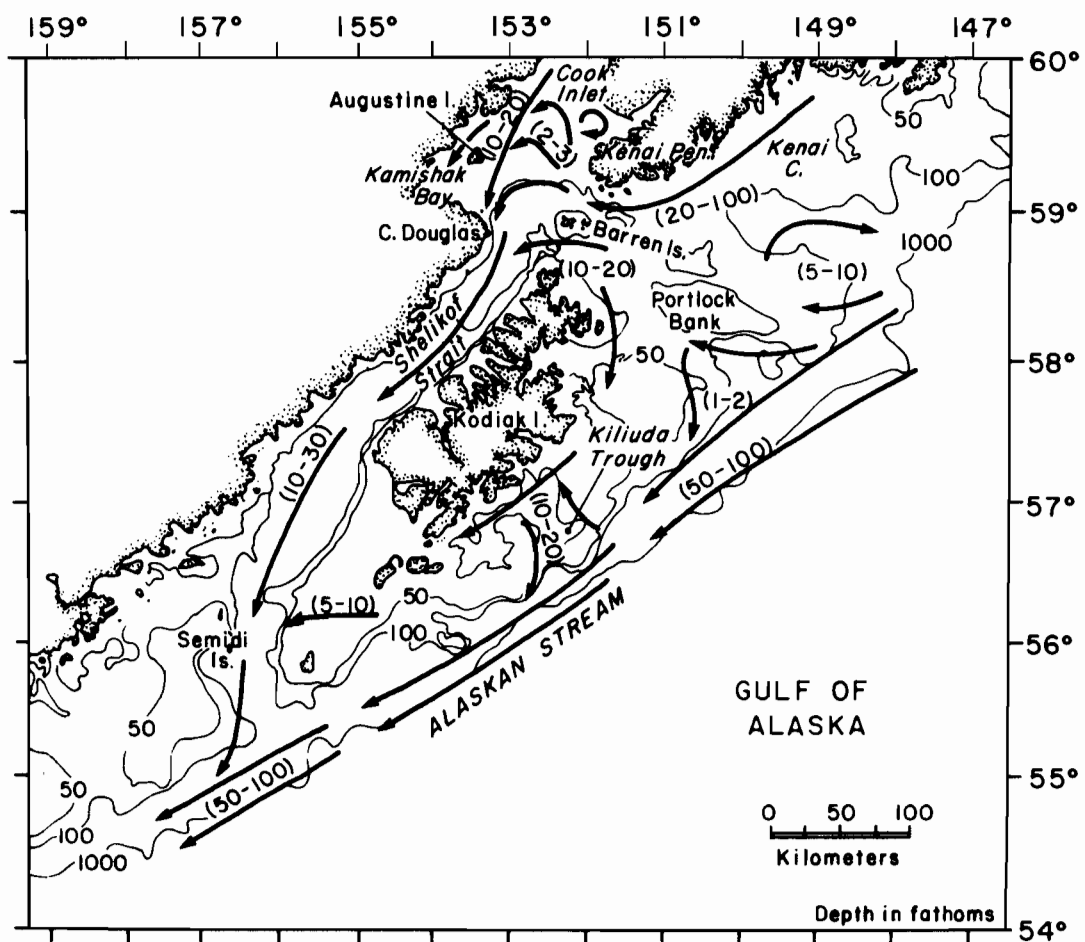


Figure 2. Schematic of near-surface currents in the northwest Gulf of Alaska region (from Muench and Schumacher, 1980), with currents in the lower Cook Inlet region derived from Muench, Mofjeld, and Charnell (1978). Numbers in parentheses give approximate range of current speeds at that location in cm/s; see text for relation between maximum/minimum values and season.

times of the year an appreciable flow occurs through lower Cook Inlet as the Kenai Current (Schumacher and Reed, 1980).

Regional meteorology is dominated by the Aleutian atmospheric low-pressure system. Winter intensification of this system results in northeasterly migration of intense low-pressure cells, manifested as cyclonic storms, along the shelf break region southeast of Kodiak Island. These storms lead to easterly winds along the coast. Weakening of the Aleutian Low in summer leads to a decrease in storm frequency and intensity; consequently local winds become weak and variable. Air temperatures are frequently below 0°C in winter, but rise to well above freezing in summer. A summary of climatological data for the northern Gulf of Alaska has been prepared by Brower and others (1977).

Within the lower Cook Inlet region, rugged land topography exerts a marked control over local winds and leads to complex flow patterns (Macklin and others, 1979). Winds in lower Cook Inlet show preferred directional channeling through gaps in the surrounding mountains formed by Cook Inlet-Shelikof Strait and Kamichak Bay (and an associated gap in the mountains to the west), and Kennedy and Stevenson entrances. It is impossible, as a consequence of the complex interactions between wind and topography, to predict winds in lower Cook Inlet on the basis of knowledge of the large-scale wind field.

Freshwater input affecting lower Cook Inlet is derived both from coastal runoff east of Kennedy Entrance, as discussed by Schumacher and Reed (1980), and from river input into upper Cook Inlet. Gauged river input to upper Cook Inlet attains a maximum mean value in excess of 2500 m<sup>3</sup>/s in June-August and is an order of magnitude smaller during the winter months of November-April (Muench et al., 1978).

Sea ice does not appear to play a significant role in the physical oceanography of lower Cook Inlet. It forms primarily in the upper Inlet, where low winter air temperatures and a relatively high freshwater content combine to create conditions favorable to ice formation. This ice is then advected southward in the western lower Inlet by the currents, sometimes being found as far south as Cape Douglas. During particularly severe winters, ice may additionally form locally in embayments such as Kachemak and Kamishak bays.

## 2. Past Research

Previous knowledge of the water circulation in Cook Inlet has been limited because measurements were insufficient to define the mean flow field. Early field observational efforts were related to pollution from industrial activities and were confined primarily to the upper portion of the Inlet (e.g., Kinney and others, 1970a; 1970b). Studies related to fisheries resources have used surface drifter trajectories to estimate the near-surface circulation in Kachemak Bay (Knull and Williamson, 1969) and in the lower Inlet (Burbank, 1977). Landsat data, which can qualitatively indicate the presence of suspended sediments in surface waters, have led to estimates of surface circulation patterns in Cook Inlet (Wright and others, 1973; Gatto, 1976). A numerical model was constructed for the tides in Cook Inlet by Matthews and Mungall

(1972); this model focused, however, upon the upper Inlet and did not provide adequate resolution of tidal currents in the lower Inlet. Most recently Muench, Mofjeld, and Charnell (1978) used current, temperature, and salinity data obtained in 1973 by the National Ocean Survey of NOAA to qualitatively discuss nontidal circulation and hydrography in the lower Inlet. They characterized mean circulation as dominated by two primary currents: a westerly flow inward through Kennedy and Stevenson entrances across the lower Inlet and out through Shelikof Strait, and a southerly flow in the western lower Inlet driven by freshwater input to the upper Inlet (see fig. 2). Outside these two major flows, mean currents were characterized as weak and variable. The mean currents had large superposed fluctuations with time scales of several days, but the data were inadequate to define the nature and source of these fluctuations.

### 3. Observation Program

#### 3.1 Current Meter Moorings

Our analysis utilizes current data obtained from taut-wire moorings (fig. 3). Geographical coordinates of each mooring, observation depths, deployment dates, record lengths, and basic record statistics are given in table 1. Aanderaa Model RCM-4 current meters with sampling intervals of 15 or 20 minutes were used. Raw data were filtered to remove high-frequency noise; this filter passed more than 99% of the amplitude at periods greater than 5 hrs, 50% at 2.86 hrs and less than 0.5% at 2 hrs. The resulting series were then either used for tidal analyses as discussed below or further filtered to remove the tidal energy. The second filter passed more than 99% of the amplitude at periods greater than 55 hrs, 50% at 35 hrs and less than 0.5% at 25 hrs. Details of this processing are discussed in Charnell and Krancus (1976).

Surface wave-induced contamination of the uppermost current records on each mooring, as discussed by Halpern and Pillsbury (1976) and Mayer, Hansen, and Ortman (1979) did not appear to be significant in our records. Consecutive 29-day tidal analyses were run for several moorings in the northern Gulf of Alaska (Pearson, Schumacher, and Muench, 1981). Computed  $M_2$  speeds showed a statistically insignificant summer-winter difference, implying that the seasonally averaged, low-frequency currents were not significantly affected by wave-induced mooring noise.

#### 3.2 Satellite-Tracked Drifters

Surface buoys having subsurface window-shade drogues were deployed upstream from (to the east of) lower Cook Inlet and tracked through the Inlet. The buoys were fiberglass spars about 5 m long attached to 2-m x 10-m window-shade drogues by 30-m nylon tethers to yield a center of drogue resistance near a depth of 35 m. Location was determined to within about 4 km by means of the Random Access Measurements System of the Nimbus-6 satellite (Levanon, 1975). Because of ambiguities in the locating mechanism and additional errors such as fluctuations in satellite orbit, the positions were passed through a subjective analysis routine (Royer et al., 1979) which resulted in a set of trajectories retaining time scales of about two days but in which tidal, inertial, and other rapid accelerations were suppressed.

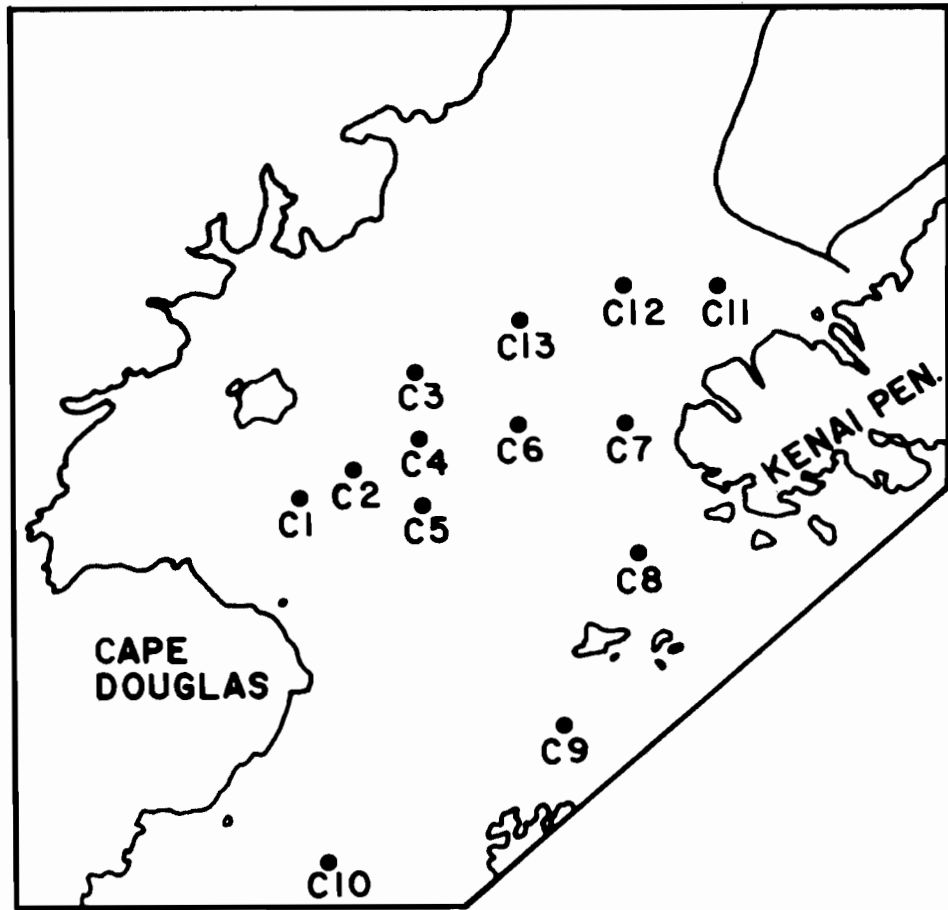


Figure 3. Location of taut-wire current moorings deployed in the lower Cook Inlet region during 1977-1978.

### 3.3. Wave Radar (CODAR) Observations

Surface currents were investigated using a doppler-shift radar method which was described in detail by Barrick, Evans, and Weber (1977). This method utilized the doppler shift of surface waves under the effect of a current to derive an instantaneous picture of surface currents over a wide area, an observation virtually impossible by other means. These observations encompassed the region just off Kachemak Bay and the area between Cape Douglas and Augustine Island. They were short in duration compared to the moored current measurements, one week or less, and provided both instantaneous and daily mean values of surface currents.

### 3.4 Temperature and Salinity Observations

Temperature and salinity data were obtained from shipboard using Plessey Model 9040 conductivity/temperature/depth profiling systems. Data were recorded during the downcast, and descent rate was held to 0.5 m/s to minimize error due to thermal sensor lag. The data were calibrated at frequent intervals using reversing thermometers and a portable shipboard salinometer calibrated with standard seawater.

## 4. Discussion

### 4.1 Mean Circulation and Seasonal Variations

Mean current speeds and directions have been computed for each deployment period using the low-pass (35-hr) filtered data (table 1 and figs. 4-5). It is apparent upon comparison between figures 4-5 and figure 2 that these observations support the circulation pattern proposed, based upon limited data obtained in summer 1973, by Muench, Mofjeld, and Charnell (1978). In addition, they provide speeds which can be used to quantify the lower Inlet flow regimes.

The prominent circulation feature was the westerly current entering the lower Inlet via Kennedy and Stevenson entrances, roughly paralleling the 100-m isobath across the lower Inlet, then exiting the Inlet through Shelikof Strait. The highest mean current speeds observed in the lower Inlet (20-30 cm/s) occurred in this current during winter 1977-78 (fig. 4); speeds were only slightly less during summer (fig. 5). In addition to the westward flow, a well-defined secondary circulation feature was present throughout the year as a southward current in the western lower Inlet; summer speeds in this current were about 20 cm/s, while winter speeds were about half this value. Compared with these two current systems, circulation in the eastern half of the lower Inlet off Kachemak Bay and the Kenai Peninsula was sluggish, with current speeds of 14 cm/s and a weakly defined northward drift at the easternmost moorings. Currents showed a pronounced tendency to parallel isobaths and thus conserve potential vorticity, as hypothesized by Muench, Mofjeld, and Charnell (1978).

The data were inadequate to observe vertical shear, because at all moorings except C10B the lower meter was sufficiently close to the bottom to place it within the influence of the benthic boundary layer (cf. Bowden, 1978). These near-bottom current observations probably reflected a frictional influence not related to forcing mechanisms for

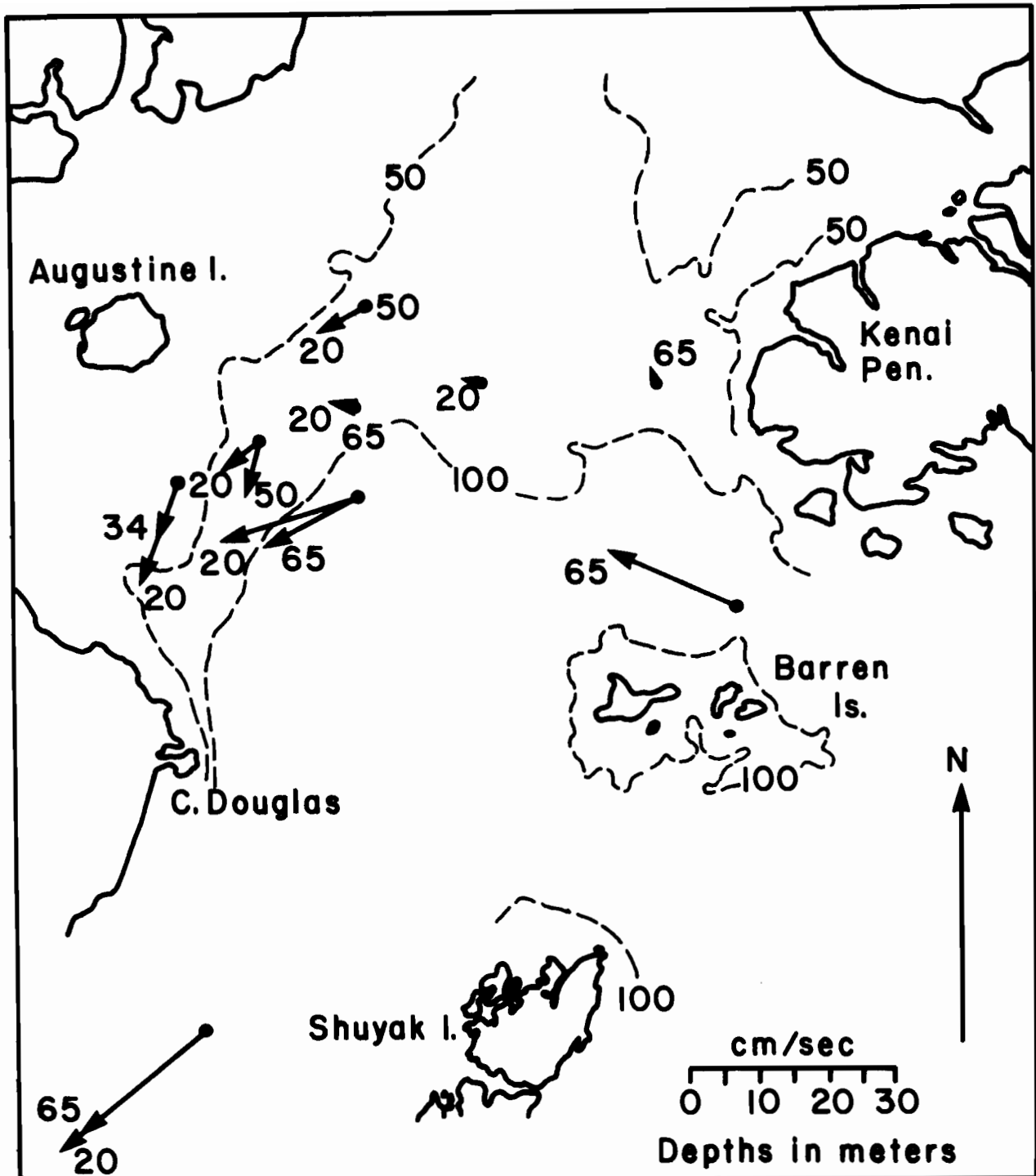


Figure 4. Mean current vectors for October 1977 through March 1978. Lengths of arrows indicate current speeds, orientation indicates direction, and numbers near arrowheads indicate observation depths in m.

Table 1. Data for lower Cook Inlet current moorings.\*

mooring	latitude N	longitude W	obs. depth	bottom depth	Winter							
					deployment date	record length	35-hr mean drift	35-hr mean dir (°T)	2.86-hr mean speed	35-hr mean speed	2.86-hr variance	35-hr variance
C1A	59.18	153.30	20	42	77-279	160	16	199	39	17	247	91
C1A	59.18	153.30	34	42	77-279	160	9	199	25	11	147	52
C2A	59.23	153.03	20	64	77-279	128	8	227	35	12	257	65
C2A	59.23	153.03	50	64	77-279	21	10	197	25	28	164	79
C3A	59.40	152.89	20	59	77-280	159	8	234	46	10	380	27
C3A	59.40	152.89	50	59	77-280	159	2	230	28	4	212	9
C4A	59.28	152.90	20	84	77-280	159	3	273	40	9	317	48
C4A	59.28	152.90	65	84	77-280	159	2	239	26	7	217	34
C5A	59.17	152.94	20	128	77-280	159	21	250	35	24	270	163
C5A	59.17	152.94	65	128	77-280	159	16	240	31	19	148	88
C6A	59.30	152.64	20	71	77-280	162	2	275	46	9	444	67
C7A	59.32	152.20	65	71	78-281	118	2	353	53	4	902	8
C8A	59.04	152.06	65	191	77-277	19	27	294	53	29	867	96
C10A	58.50	153.19	20	170	77-278	159	28	230	33	31	471	383
C10A	58.50	153.19	65	170	77-278	159	23	229	27	26	295	254

NOTE: Data include latitude (N), longitude (W), observation depth (m), bottom depth (m), deployment date (year, Julian Day), length of record (days), speed and direction of mean 35-hr filtered current (cm/s and °T), 2.86-hr and 35-hr filtered mean speeds (cm/s), and 2.86-hr and 35-hr filtered variance (cm<sup>2</sup>/s<sup>2</sup>).

\* Mooring locations are indicated in figure 3.



Table 1. Continued

mooring	latitude N	longitude W	obs. depth	bottom depth	<u>Summer</u>							
					deployment date	record length	35-hr mean drift	35-hr mean dir (°T)	2.86-hr mean speed	35-hr mean speed	2.86-hr variance	35-hr variance
C1B	59.18	153.31	18	40	78-148	87	9	204	32	10	163	28
C1B	59.18	153.31	35	40	78-148	143	4	193	18	6	84	15
C2B	59.23	153.13	18	62	78-148	143	15	218	41	17	416	84
C3B	59.41	152.89	25	64	78-148	143	17	232	52	19	604	55
C3B	59.41	152.89	55	64	78-148	97	1	95	25	4	180	8
C4B	59.28	152.92	19	83	78-150	138	3	246	26	6	552	27
C4B	59.28	152.92	64	83	78-150	141	1	158	27	7	199	29
C5B	59.17	152.90	27	135	78-148	115	19	252	45	23	797	258
C5B	59.17	152.90	127	135	78-148	123	2	200	15	6	85	23
C6B	59.31	152.63	26	77	78-148	142	1	256	46	7	519	39
C6B	59.31	152.63	71	77	78-148	143	3	119	25	5	193	12
C7B	59.31	152.18	17	68	78-148	142	4	310	72	7	1505	42
C7B	59.31	152.18	62	58	78-148	142	2	237	39	4	598	5
C8B	59.03	152.06	63	190	78-149	138	22	287	62	24	1608	354
C8B	59.03	152.06	179	190	78-149	138	8	259	40	9	262	20
C9B	58.78	152.27	66	124	78-149	138	11	300	53	13	966	103
C9B	58.78	152.27	114	124	78-149	138	11	301	34	12	363	75
C10B	58.50	153.20	25	175	78-148	134	14	222	20	18	183	118
C10B	58.50	153.20	70	175	78-148	134	12	221	17	15	120	94
C10B	58.50	153.20	165	175	78-148	134	4	200	11	9	67	49
C11A	59.56	151.66	82	87	78-149	20	1	334	10	2	14	1
C12A	59.53	152.23	20	50	78-148	81	4	42	55	5	991	4
C12A	59.53	152.23	46	50	78-148	141	4	30	43	5	652	4
C13A	59.47	152.68	26	68	78-148	141	5	189	60	9	704	22



the flow. Variations in flow direction with depth appeared to be small, at locations where mean speeds were high, except at moorings C5B, C8B, and C10B where near-bottom currents were rotated 2050° to the left of the overlying flow. These directional deviations were in the correct sense to be a combination of veering caused by the benthic boundary layer and bathymetric steering. There appeared to be no consistent directional relationship between upper- and lower-level currents in the eastern lower Inlet, where flow was sluggish.

Seasonal variations in the currents in lower Cook Inlet were pronounced. The westerly mean flow through the region was about twice as great in winter as during summer at mooring C10 in northern Shelikof Strait, but this difference was not evident within the same flow regime farther east either in central lower Cook Inlet (C5). Summer current speeds at the latter location are probably heavily influenced by the summer flow maximum in the Kenai Current. This current is baroclinic and attains peak speeds in September-October (Schumacher and Reed, 1980). It is also only 1015 km wide, and would not necessarily be fully reflected at mooring C10 in the center of Shelikof Strait, about 20 km offshore. The large winter mean current speed resulted from midwinter wind-driven coastal convergence and possibly from increased barotropic flow in the Gulf of Alaska gyre which would be expected, through its associated alongshore sealevel slope. A similar mechanism has been suggested for mean flow in the mid-Atlantic Bight (Beardsley and Winant, 1979). The bimodal nature of the winter and late summer flow peaks shows clearly in figure 6, which presents the 7-day averaged current speeds from mooring C10; the October runoff-driven peak is evident in both 1977 and 1978, as is the February-March 1978 peak driven by increased alongshore wind stress (Schumacher and Reed, 1980). A period of relatively low current speeds (1520 cm/s) occurred during the November-December 1977 period between the two maxima. Minimum speeds of 510 cm/s occurred during June-August 1978, a period during which both baroclinic and barotropic forcing of the southwestward, alongshore flow were small.

Seasonal variations were present also in the southerly flow which occupied the western lower Inlet. Just seaward of the 50-m isobath (moorings C2 and C3), summer current speeds were nearly twice as great as in winter (about 16 as compared to 8 cm/s). The inverse was true shoreward of 50 m (mooring C1). Increased summer flow at C2 and C3 was a consequence of larger freshwater input to the upper Inlet during summer and autumn than during winter. It is unclear why the summer speed increase at C2 and C3 was not reflected at C1. The increase may reflect an offshore migration of the core of the southerly flowing current, so that C1 during summer fell shoreward of the locus of maximum current speeds. Moorings C2 and C3 behaved similarly because they lay along the same isobath (about 69 m).

Data from the area of sluggish flow in the eastern lower Inlet were inadequate to define seasonal differences because too few data were obtained there during winter. Observations from the upper layer (17-26 m, depending upon the specific mooring) suggest, however, that speeds were higher by about a factor of two in summer than during winter. This would be consonant with higher current speeds during summer caused by the Kenai Current.

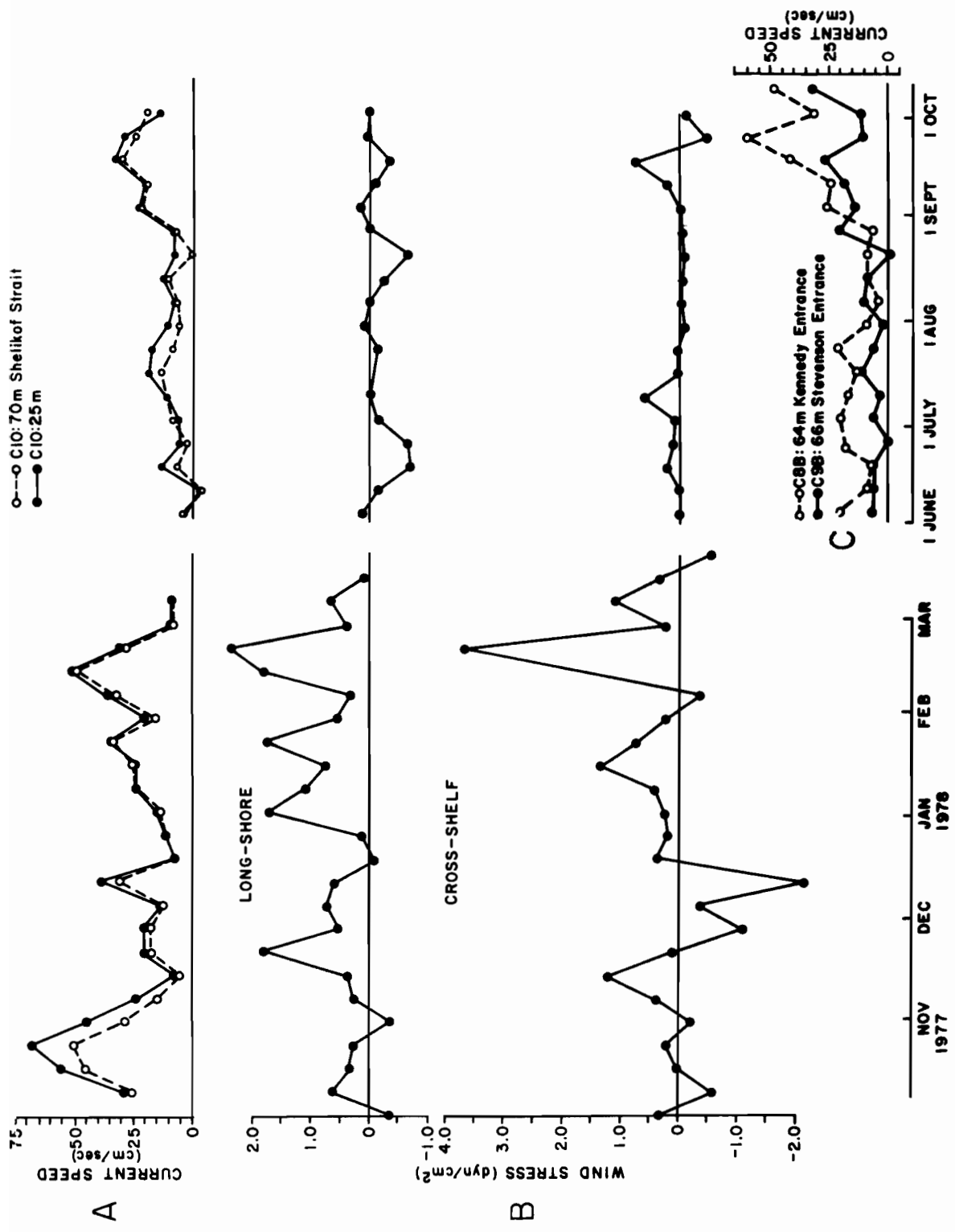


Figure 6. Seven-day mean current speeds at middepths (65-70 m) and near-surface (20-25 m) in northern Shelikof Strait at mooring C10 (after Schumacher and Reed, 1980). Mooring location is indicated on figure 3.

## 4.2 Low-Frequency Current Fluctuations

Prominent low-frequency fluctuations were superposed on the mean flow in the lower Cook Inlet region. These fluctuations had time scales of 1-2 weeks and magnitudes of the same order as, and at times greater than, the mean flow. They affected both speed and direction, though in the regions of strong mean flow the effect was primarily on speed with little directional deviation. The nature of the fluctuations is illustrated in the representative time-series segments of several records from lower Cook Inlet (figure 7); they are also evident in the 7-day mean speeds shown on figure 6. Computations of horizontal kinetic energy reveal that in the region of strong westerly flow about 50% of the nontidal energy was contained in low-frequency fluctuations. In lower Cook Inlet north of the westerly flow, 80-90% of the nontidal energy was contained in the fluctuating flow. The fluctuations therefore exerted a dominant effect upon instantaneous currents. At mooring C5, for example (fig. 7), directional variations of nearly 90° and speeds of up to about 75 cm/s were associated with these fluctuations. At mooring C4, which during summer indicated virtually zero mean flow, instantaneous currents were controlled entirely by the fluctuating and tidal components.

The distribution of low-frequency horizontal kinetic energy in lower Cook Inlet indicates that the fluctuations were associated with the prominent westerly flow (fig. 8). The greatest low-frequency horizontal kinetic energy ( $>200 \text{ cm}^2/\text{s}^2$ ) was present in this westerly flow, except in Stevenson Entrance where values were about half this. Values dropped off sharply northward into the Inlet to less than  $100 \text{ cm}^2/\text{s}^2$ . Within the lower Inlet north of the 100-m isobath, values were highest ( $60\text{-}70 \text{ cm}^2/\text{s}^2$ ) in the western portion and decreased monotonically eastward to a low of  $4 \text{ cm}^2/\text{s}^2$  off Kachemak Bay.

While it is possible to identify the westerly current as the probable locus of low-frequency fluctuations, comparisons between the different moorings revealed a confused pattern of correlation between fluctuations at different locations. For example, a northerly flow event on about 25 October 1977 at moorings C1, C2, and C4 (fig. 7) was not reflected in records from the other moorings. Records from mooring C3, in particular, showed little correlation with events elsewhere in the lower Inlet. As a quantitative check of the results of these visual correlations, horizontal coherencies were computed between the 20-m current records; the resulting coherencies were uniformly low, in support of the visual correlation results.

As for the horizontal case, both visual inspection and coherency computations yielded inconsistent results for vertical correlations. The currents were vertically highly coherent at mooring C1, whereas at C3 and C4 there was virtually no vertical coherency. Other moorings fell between these extremes, but showed no detectable pattern of horizontal variation.

The source of the low-frequency fluctuations observed in lower Cook Inlet is uncertain. Comparison between selected major flow events and meteorological parameters was inconclusive, primarily because the latter parameters were too incomplete to yield a meaningful comparison. An

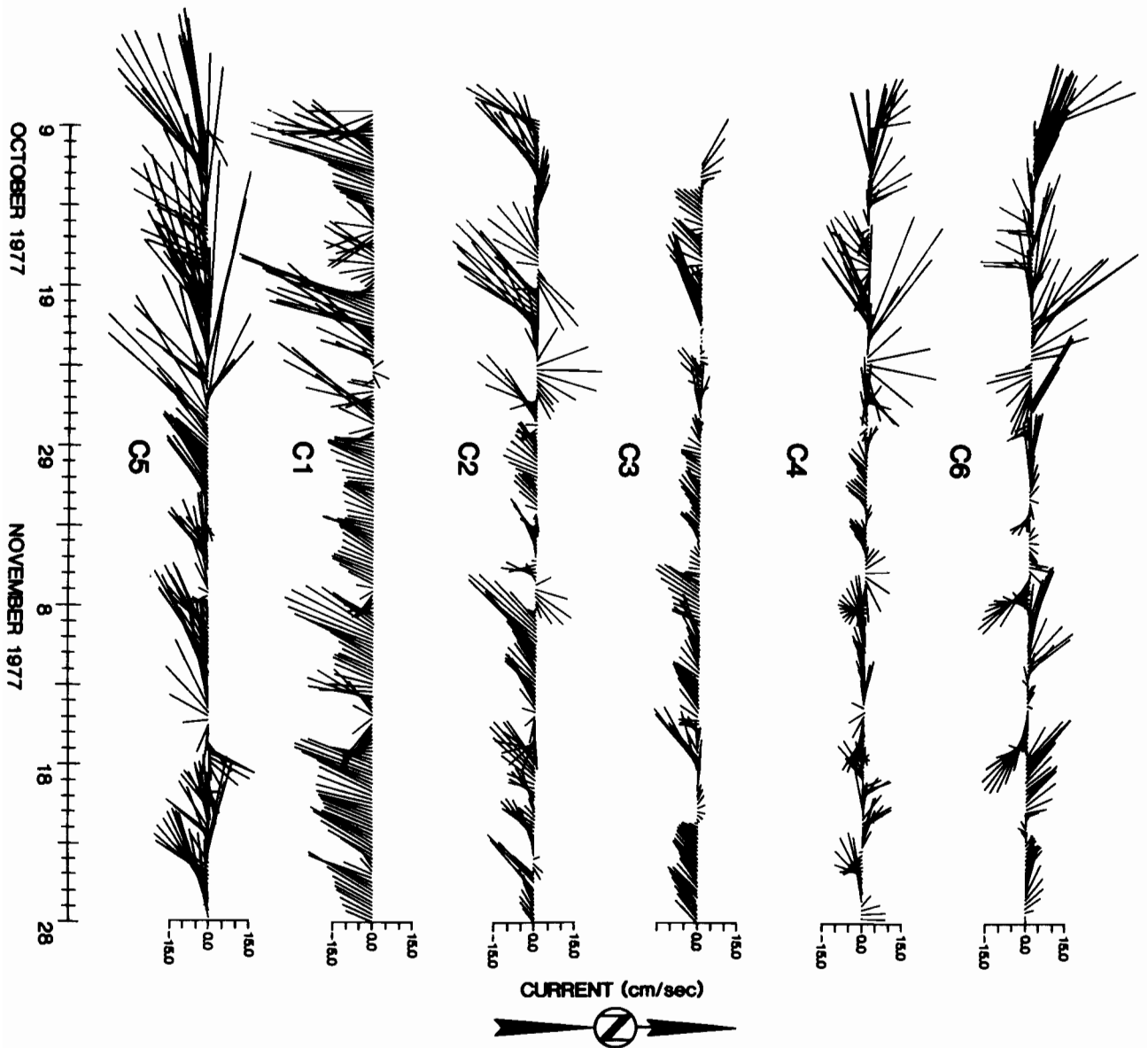


Figure 7. Representative segments of low-pass (35-hr) filtered currents from six locations at 20-m depth. Mooring locations are indicated on figure 3.

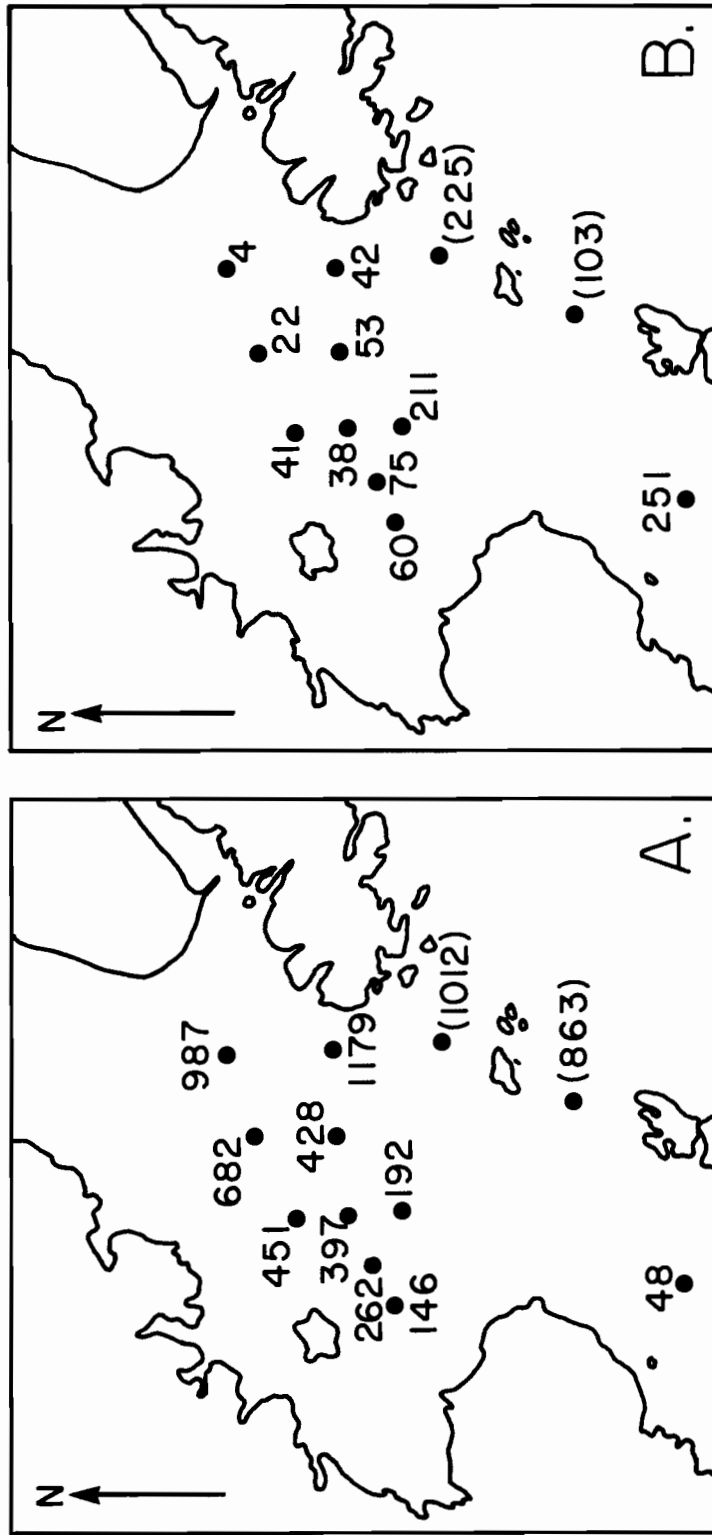


Figure 8. Mean distribution of horizontal kinetic energy ( $\text{cm}^2/\text{s}^2$ ) at 20- to 25-m depths in two frequency bands; A) 0.03-0.35 cph, which includes semidiurnal and diurnal tidal and inertial energy, and B) 0.001-0.03 cph, which includes prominent low-frequency fluctuations. Parenthesized values were obtained from 63- to 66-m deep observations rather than from 20-25 m.

environmental buoy moored in the lower Inlet and intended to provide meteorological data for comparison with the current records malfunctioned, and the complex local interaction between winds and topography precluded use of the regional atmospheric pressure fields to deduce winds over the lower Inlet. Research on other embayments has shown that these fluctuations are a common feature, and that such systems are strongly responsive to atmospheric forcing on the outlying continental shelf (Wang and Elliott, 1978; Wang, 1978; Winant and Beardsley, 1979; Holbrook, Muench, and Cannon, 1980). Such forcing is clearly present off lower Cook Inlet in the form of cyclonic low-pressure storms which migrate northeastward in the Gulf of Alaska. It is also possible that flow fluctuations may be driven by the cross-shelf propagation of meso-scale eddies or meanders associated with the highly energetic Alaskan Stream, which follows the shelf break south of Kodiak Island. Data from the Alaskan Stream are, however, inadequate to test this hypothesis.

#### 4.3 Tidal Currents

The tidal currents in lower Cook Inlet are of the mixed type, primarily semidiurnal ( $M_2$ ). The highest currents occurred in Kennedy and Stevenson entrances (moorings C8 and C9), where  $M_2$  amplitudes were about 70 cm/s. Within the lower Inlet farther north, currents were higher in the eastern part (about 100 cm/s at mooring C7) than in the western portion (30-40 cm/s at C1-C4). No evidence was found of the extremely low tidal currents reported for one station in central lower Cook Inlet by Muench, Mofjeld, and Charnell (1978). The currents were oriented approximately parallel to the axis of the Inlet. There is an antinode in the  $M_2$  tidal wave in northern Shelikof Strait, where the wave entering lower Cook Inlet around the north end of Afognak Island meets the wave that has entered the system via the south end of Shelikof Strait. This antinode is located close to mooring C10, consequently, the  $M_2$  current at C10 was extremely weak (about 8 cm/s) relative to those elsewhere in the region.

The diurnal ( $K_1$ ) tidal current exhibited more uniform and lower speeds (5-10 cm/s) than the  $M_2$ . As for the  $M_2$  tide, there was an antinode in northern Shelikof Strait which led to extremely weak  $K_1$  currents (about 2 cm/s) at mooring C10.

The tendency for tidal currents to be larger in the eastern than in the western lower Inlet is demonstrated in Figure 8A. The energy in the tide-containing band was as much as five times greater in the eastern than in the western Inlet, and about twenty times larger in Kennedy Entrance than in northern Shelikof Strait near the  $M_2$  and  $K_1$  antinodes.

#### 5. Summary

The major mean circulation feature in the lower Cook Inlet region is the westerly flow. This can be graphically summarized by reference to two additional sources of data; trajectories from satellite-tracked, drogued buoys which were followed through the system in summer 1978 (fig. 9) and the results of an experiment carried out in July 1976 using a doppler-shift wave radar method (fig. 10). Drogue 1775 closely followed isobaths through the lower Inlet to a point off Cape Douglas, while drogue 1421 entered through Kennedy Entrance and showed primarily



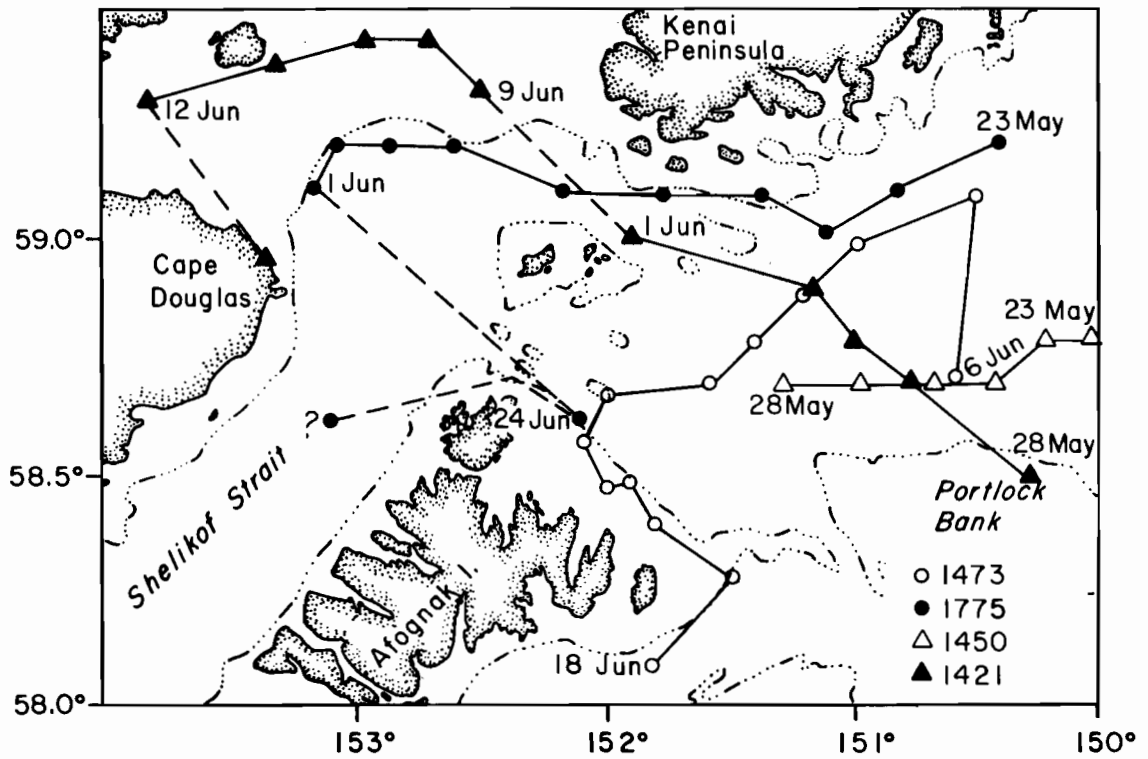


Figure 9. Trajectories of drogued, satellite-tracked buoys deployed in 1978. Locations are plotted at 1-day intervals.

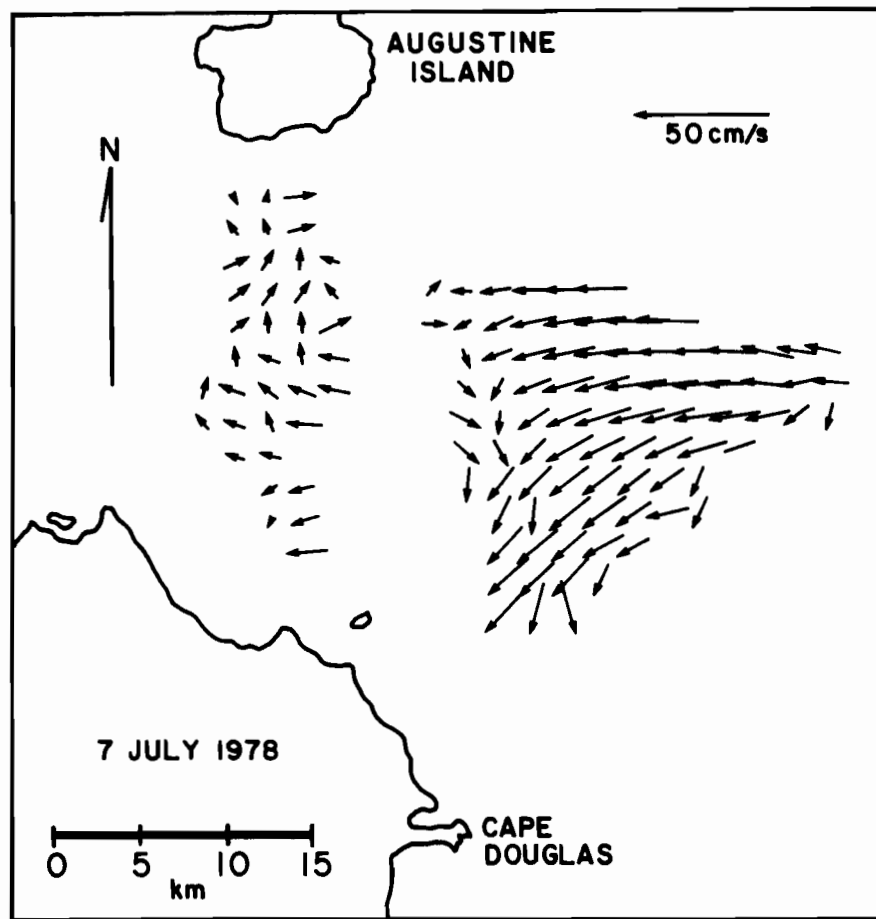


Figure 10. Example of 24-hr mean surface currents observed in July 1978 using the doppler-shift radar unit discussed by Barrick, Evans, and Weber (1977). Data are courtesy of Dr. A.S. Frisch (Wave Propagation Laboratory, NOAA).

westward movement and some cross-isobath flow to the northward. Both these drogues showed mean speeds of about 15 cm/s, in rough agreement with that which would be predicted from the moored current observations. Drogue 1473 did not enter the lower Inlet, possibly in response to an easterly flow pulse similar to those observed on the current records in Stevenson Entrance. The 24-hour mean surface current picture compiled using wave radar data defined circulation off Cape Douglas, where the westerly flow is constrained by the bathymetry to curve southward and join the southward flow from the upper Inlet, creating particularly strong currents.

The well-documented westerly flow through the lower Inlet had superposed upon it tidal and lower frequency fluctuating currents whose magnitude varied with location. Both were maximum in Kennedy and Stevenson entrances, and decreased to the north and west. Tidal currents were minimum in northern Shelikof Strait, and were larger in eastern than in western lower Cook Inlet. Low-frequency fluctuation decreased northward. This is illustrated on figure 8 and in table 1, where the 2.86-hr variance represents primarily tidal currents and the 35-hr variance represents low-frequency fluctuations.

Near-bottom current speeds at a given location are of interest to sediment transport. Mean speeds, averaged over the entire length of the record and including tidal currents, are given in table 1 as "2.86-hr mean speed." These were generally above about 25 cm/s, with values of about 25 cm/s in the western portion of the lower Inlet and about 50 cm/s in the eastern portion and in Kennedy and Stevenson entrances. This parallels the distribution of energy in tidal bands closely; thus, we conclude that tides are a major contributor to the relatively high near-bottom current speeds observed.

The tidal fluctuating currents generally paralleled the channel orientation (table 2). In most cases, current directions for the different components were approximately aligned. In some cases (e.g., mooring C1), however, the lesser components were directed up to 90° away from the major  $K_1$  and  $M_2$  currents. The low-frequency fluctuations tended to be aligned with the mean flow in regions of strong mean currents (fig. 7). Elsewhere, they appeared to be random in orientation and frequently described full 360° rotations of the current vector.

Table 2. - Tidal current components for four major species derived from current data using the Munk-Cartwright response method (Munk and Cartwright, 1966); H is current amplitude (cm/s), G is phase relative to Greenwich ( $^{\circ}$ ), D is direction of major axis ( $^{\circ}$ ), and R is sense of rotation (C for clockwise, A for anticlockwise).

Station	Meter Depth (m)	$O_1$			$K_1$			$S_2$			$M_2$										
		H	Major G	Minor D	H	Major G	Minor D	H	Major G	Minor D	H	Major G	Minor D								
C1B	18	3.6	237	34	3.4	C	6.5	229	323	4.8	C	13.6	294	313	5.9	C	33.2	161	306	19.1	C
C2A	20	6.3	241	15	2.8	C	9.4	257	5	4.3	C	14.0	324	345	6.8	C	36.5	300	353	20.7	C
C3A	20	5.4	239	26	3.8	C	11.6	243	16	5.7	C	19.8	324	3	8.2	C	53.4	303	7	24.6	C
C4A	20	6.3	222	14	2.3	C	9.7	242	4	3.7	C	16.8	330	355	6.2	C	46.3	302	357	18.9	C
C5A	20	3.9	192	355	0.3	A	5.4	222	344	0.5	A	10.2	326	338	0.9	C	28.0	297	338	4.5	C
C6B	26	6.9	199	8	2.8	C	11.4	213	359	3.7	C	22.7	315	358	7.3	C	57.3	287	356	19.5	C
C7B	17	8.9	161	358	2.6	C	15.9	184	358	2.5	C	36.8	299	358	4.8	C	98.0	269	357	17.4	C
C8B	63	8.7	179	301	3.3	A	13.1	207	302	3.7	A	28.0	307	300	2.5	C	70.0	278	295	5.8	C
C9B	66	10.0	191	293	2.5	C	15.4	205	296	1.9	C	27.2	298	295	1.5	C	70.5	268	291	9.6	C
C10B	25	2.1	265	58	0.3	A	1.7	307	35	0.1	A	3.3	48	25	1.7	C	8.3	4	35	3.6	C
C12A	20	9.3	201	9	1.1	C	15.1	212	6	2.0	C	29.8	319	7	0.6	C	79.7	294	6	4.4	C
C13A	26	9.5	222	23	4.2	C	14.3	235	22	4.5	C	26.5	335	16	9.8	C	74.1	308	13	28.0	C

## 6. Acknowledgements

Only through the cooperation of many individuals, primarily those at the Pacific Marine Environmental Laboratory of NOAA, was it possible to successfully carry out the extensive field program and subsequent data processing and analysis leading to this manuscript. Special thanks are extended to Jim Haslett, Dick Carlone, and Bill Parker, whose dedication to duty ensured the success of the mooring operations, and to Sharon Wright and Lynn Long for aiding in the data processing.

This study was supported in part by the Bureau of Land Management through interagency agreement with the National Oceanic and Atmospheric Administration under which a multiyear program responding to needs of petroleum development of the Alaskan continental shelf is managed by the Outer Continental Shelf Environmental Assessment Program (OCSEAP) office, and in part by the Pacific Marine Environmental Laboratory, NOAA.

## 7. References

- Barrick, D.E., Evans, M.W., and Weber, B.L., 1977, Ocean surface currents mapped by radar: *Science*, v. 198, p. 138-144.
- Beardsley, R.C., and Winant, C.D., 1979, On the mean circulation in the Mid-Atlantic Bight: *J. Phys. Oceanogr.*, v. 9, p. 612-619.
- Bowden, K.F., 1978, Physical problems of the benthic boundary layer: *Geophys. Surveys*, in press.
- Brower, W.A., Jr., Diaz, H.F., Prechtel, A.S., Searby, H.W., and Wise, J.L., 1977, Climatic Atlas of The Outer Continental Shelf Waters and Coastal Regions of Alaska, Vol. 1, Gulf of Alaska: NOAA/OCSEAP Final Rept. RU No. 347. (unpub. man.)
- Burbank, D.C., 1977, Circulation studies in Kachemak Bay and lower Cook Inlet, Alaska: Dept. of Fish and Game, Anchorage, Alaska. (unpub. man.)
- Charnell, R.L., and Krancus, G.A., 1976, A processing system for Aanderaa Current Meter data: NOAA Tech. Memo. ERL PMEL-6.
- Favorite, F., 1967, The Alaskan Stream: Bull. 21, Int'l. N. Pac. Fish. Comm., Vancouver, B.C.
- Favorite, F., 1974, Flow into the Bering Sea through Aleutian Island passes: In Hood, D.W., and Kelley, E.J., eds., *Oceanography of the Bering Sea, With Emphasis on Renewable Resources*: Univ. of Alaska Occas. Publ. No. 2, Fairbanks, Alaska, p. 3-37.
- Gatto, L.W., 1976, Baseline data on the oceanography of Cook Inlet, Alaska: Rept. 76-25, U.S. Army Cold Regions Res. and Engr. Lab., Hanover, N.H.
- Halpern, D., and Pillsbury, R.D., 1976, Influence of surface waves on subsurface current measurements in shallow water: *Limn. and Oceanogr.*, v. 21, p. 611-616.
- Holbrook, J.R., Muench, R.D., and Cannon, G.A., 1980, Seasonal observations of low-frequency atmospheric forcing in the Strait of Juan de Fuca: In Freeland, H.J., and Farmer, D.M., eds., *Fjord Oceanography*: Plenum Press, N.Y., p. 305-317.
- Kinney, P.J., Button, D.K., Schell, D.M., Robertson, B.R., and Groves, J., 1970[a], Quantitative assessment of oil pollution problems in Alaska's Cook Inlet: Rept. R-169, Inst. Mar. Sci., Univ. of Alaska, Fairbanks, Alaska.
- Kinney, P.J., Groves, J., and Button, D.K., 1970[b], Cook Inlet environmental data, R.V. Acona cruise 065 May 21-28, 1968: Rept. R70-2, Inst. Mar. Sci., Univ. of Alaska, Fairbanks, Alaska.

- Knoll, J.R., and Williamson, R., 1969, Oceanographic survey of Kachemak Bay, Alaska: Man. Rept. 60, Bur. Comm. Fish. Lab., Auke Bay, Alaska.
- Levanon, N., 1975 (ed.), Special issue on data collection from multiple earth platforms: IEEE Trans. on Geoscience Electronics, v. 13.
- Macklin, S.A., Lindsay, R.W., Reynolds, R.M., and Muench, R.D., 1979, Observations of mesoscale winds in an orographically-dominated estuary: Cook Inlet, Alaska: Proc. XVII General Assembly of the IUGG, IAPSO Circular, Canberra, Australia, p. 111.
- Matthews, J.B., and Mungall, J.C.H., 1972, A numerical tidal model and its application to Cook Inlet, Alaska: J. Mar. Res., v. 30, p. 27-38.
- Mayer, D.A., Hansen, D.V., and Ortman, D.A., 1979, Long-term current and temperature observations on the Middle Atlantic shelf: J. Geophys. Res., v. 84, p. 1776-1792.
- Muench, R.D., Mofjeld, H.O., and Charnell, R.L., 1978, Oceanographic conditions in lower Cook Inlet; spring and summer 1973: J. Geophys. Res., v. 83, p. 5090-5098.
- Muench, R.D., and Schumacher, J.D., 1980, Physical oceanographic and meteorological conditions in the northwest Gulf of Alaska: NOAA Tech. Memo. ERL PMEL-22, 147 pp.
- Munk, W.H., and Cartwright, D., 1966, Tidal spectroscopy and prediction: Phil. Trans. Royal Soc. London A, v. 259, p. 533-581.
- Ohtani, K., 1970, Relative transport in the Alaskan Stream in winter: J. Oceanogr. Soc. Japan, v. 26, p. 271-282.
- Pearson, C.A., J.D. Schumacher and R.D. Muench, 1981, Effects of wave-induced mooring noise on tidal and low-frequency current observations, Deep-Sea Res., v. #28A (in press).
- Reed, R.K., 1980, Direct measurement of recirculation in the Alaskan Stream: J. Phys. Oceanog., v. 10., p. 976-978.
- Reed, R.K., and Taylor, N.E., 1965, Some measurements of the Alaska Stream with parachute drogues: Deep-Sea Res., v. 12, p. 777-784.
- Reed, R.K., Muench, R.D., and Schumacher, J.D., 1980, On baroclinic transport of the Alaskan Stream near Kodiak Island: Deep-Sea Res., v. 27, p. 509-523.
- Royer, T.C., Hansen, D.V., and Pashinski, D.J., 1979, Coastal flow in the northern Gulf of Alaska as observed by dynamic topography and satellite-tracked drogued drift buoys: J. Phys. Oceanog., v. 9, p. 785-801.

- Schumacher, J.D., and Reed, R.K., 1980, Coastal flow in the northwest Gulf of Alaska: the Kenai Current: J. Geophys. Res., v. 85, p. 6680-6688.
- Thomson, R.E., 1972, On the Alaskan Stream: J. Phys. Oceanogr., v. 2, p. 363-371.
- Wang, D.P., 1978, Subtidal sea level variations in the Chesapeake Bay and relations to atmospheric forcing: J. Phys. Oceanogr., v. 9, p. 413-421.
- Wang, D.P., and Elliott, A.J., 1978, Non-tidal variability in the Chesapeake Bay and Potomac River: evidence for non-local forcing: J. Phys. Oceanogr., v. 8, p. 225-232.
- Wright, F.F., Sharma, G.D., and Burbank, D.C., 1973, Ertis-1 observations of sea surface circulation and sediment transport, Cook Inlet, Alaska: Proc. Symp. on Significant Results Obtained From The Earth Resources Technology Satellite-1, NASA, Washington, D.C., p. 1315-1322.